ELSEVIER

Journal of Molecular Structure (Theochem) 311 (1994) 29–35

THEO CHEM

Dynamically defined reaction path (DDRP) method

M.I. Bán[a,*], Gy. Dömötör[a], L.L. Stachó[b]

[a] *Institute of Physical Chemistry, Attila József University, PO Box 105, H-6701 Szeged, Hungary*
[b] *Bolyai Institute for Mathematics, Attila József University, Aradi Vértanúk tere 1, H-6720 Szeged, Hungary*

(Received 19 July 1993; accepted 12 October 1993)

Abstract

Brief accounts of the theoretical background of the dynamically defined reaction path (DDRP) method and algorithm are presented. By employing mathematical functions used for testing reaction path-following algorithms and by simple chemical examples, applications of the procedure have been illustrated.

1. Introduction

Most of the conventional reaction path (RP) calculations [1–12] start at a saddle point (SP) and take successive steps in the direction of the negative gradient. With decreasing step sizes the calculations lead to a converged RP regarded as a minimum energy reaction path (MERP). If the coordinate system is mass-weighted, the RP is called the intrinsic reaction coordinate (IRC). The conventional RP-following algorithms are globally unstable especially when the RP is curved and/or twisted. Moreover, they are aimed at treating the differential-topological simplest case where two steepest descent paths in a reaction valley lead from an SP of rank 1 to two local minima. Such an approach tends to be problematic if the RP bifurcates or is very curved. Another disadvantage of these methods is that they cannot essentially be developed any further and cannot be run effectively on the most modern vector computers. In previous papers [13,14] we proposed a new, theoretical global searching procedure which seems to overcome these problems. The algorithm [15] developed on the basis of Theorem 2.1 in Ref. [13] and a simple computer program [16,17] based on this algorithm were tested by some very complicated artificial mathematical functions [13,15] constructed to demonstrate the high stability of the procedure, and by illustrating some traits of the H_3 system [18]. In this work, after summarizing the main features of the dynamically defined reaction path (DDRP) method and the algorithm, we present further applications showing the functioning and use of our procedure. Experiences with such complicated mathematical surfaces as determined by the functions of Müller and Brown (MB) [5] and Gonzalez and Schlegel (GS) [12] further demonstrate the efficiency and stability of the procedure. Examples of the chemical systems HHH, HHCl, HClH, ClHCl and ClClH presuming collinearity are also used to illustrate the method.

* Corresponding author.

SSDI 0166-1280(93)03530-K

2. Algorithm

One of the chief merits of Fukui's IRC concept [19] is that it provides us with quite a faithful picture of chemical reactions using geometrical considerations concerning the potential energy hypersurface (PES). Originally an IRC was defined as a piecewise smooth curve joining two local minima whose tangent vector is always orthogonal (in the mass-weighted cartesian coordinate system) to the level sets of the PES.[a] To be more precise, if $U : \mathbb{R}^n \to \mathbb{R}$ is the potential energy function then a curve $c : [a, b] \to \mathbb{R}^n$ between two local minima of U is an IRC if and only if for some scalar function $\lambda : (a, b) \to \mathbb{R}$. Note that this concept is independent of parametrization; moreover, it only depends on the level set structure of U. This latter observation has not yet been fully explored and exploited. As we shall see below in the example of the MB-surface [5], a monotonic transformation of U does not change the level sets but will drastically reduce the numerical costs of following the IRC.

The algorithm for the simplest case based on the theory described in detail in Ref. [13] is characterized by the following main steps. Given a curve connecting two local minima of the energy function, the phase flow of the negative gradient takes it to converge to some sequences of steepest descent and ascent paths between the two minima (which are not affected by the flow) under not very restrictive conditions on the energy function (see Theorem 2.1 in Ref. [13]). In practice, the successive phase curves (the "time-resolved RP") can be approximated by the aid of the following algorithm. Choose $P_1, \ldots, P_n$ to be consecutive points representing the polygon c. First calculate the effect Φ^η of the flow of $-\nabla U$ on the points for some (virtual) time η. Thus we have to calculate the solutions of the ordinary differential equation $\mathrm{d}/\mathrm{d}t\, x(t) = -\nabla U(x(t))$ with the initial values $x(0) = P_i$ for $t = \eta$. Since for large values of η the obtained points P_i' approach the set of stationary points of U, it is advisable to take only a small value for η and then to *homogenize* the polygon $P_1', \ldots, P_n'$. This can be done by placing further points onto the segments P_i', P_{i+1}' whenever the distance $\|P_i' - P_{i+1}'\|$ exceeds some given value of ε and by deleting points $P_i', P_{i+1}', \ldots, P_r'$ whenever $\sum_{j=i-1}^{r+1} \|P_j' - P_{j+1}'\| \leqslant \varepsilon$, in order to obtain an approximating polygon for the curve $\Phi^\eta(c)$ whose consecutive vertices have distances between the values $\varepsilon/2$ and ε. It is indeed not necessary to try to find a very precise approximation for the solution of the initial problems $\mathrm{d}/\mathrm{d}t\, x(t) = -\nabla U(x(t))$; $x(0) = P_i$. In most cases it is sufficient to take $P_i' \approx P_i - \eta \nabla U(P_i)$. If very large values of ∇U can occur it is advisable to use Euler's simple method of steps (see, for example, Ref. [20]) with a given maximum admissible step-length σ to construct the point P_i'. The homogenized polygon $P_1', \ldots, P_n'$ can then be used to obtain a polygon approximation of the curve $\Phi^{2\eta}(c) = \Phi^\eta(\Phi^\eta(c))$, and iterating the procedure we get the time-resolution pattern (or "stroboscopic view") of IRC in the succession of approximate polygons $\Phi^{3\eta}(c), \Phi^{4\eta}(c), \ldots$, etc. The choice of the three governing parameters ε, η and σ requires some familiarity with the function U. With "brute force" we may apply arbitrarily small values to ensure a good approximation for some IRC (this is guaranteed for $\varepsilon, \eta, \sigma \to 0$). However, if the IRC is not very curved, the use of too small ϵ-values is unnecessary and the optimum choice of η and σ can be in the order of $\varepsilon / \max \|\nabla U\|$.

In practice, first a polygon is defined in the multidimensional configurational space of the actual (chemical) problem and points are taken up on this polygon.[b] When starting the procedure, these points are determined by the vertices of the chosen polygon. In the second step, depending on the choice of parameter ε, the number of points will change: if the distance between the two neighbouring vertices is smaller or larger, respectively, than that determined by ε, points will be deleted or created on the polygon. In the third step, by executing a homogenizing procedure,

[a] Throughout this paper mass-weighted (or mass-scaled) coordinates are considered.

[b] The number of points is not determined by the number of atoms involved in the chemical reaction, although it is dependent on the mathematical (differential-topological) complexity of the PES.

uniform distribution of points will be achieved. Then the points, directed by the actual vector field generated by any quantum chemical (or other) method suitable for energy calculations, will be moving on the PES. After a number of iterations, a new approximate polygon is generated from the former one and simultaneously the previous uniform distribution of the points will be changing: near the SP the number of points will be becoming exhausted and towards the minima the points will be crowding. So again a homogenization must follow to ensure the uniform distribution of points thus facilitating the generation of a following new polygon.[c] Consequently, the two main steps, namely (i) the determination of a new polygon and (ii) the homogenization of the points of the new polygon, will be carried out alternately until the procedure converges. In fact, the frequency of iteration cycles commencing always with the generation of a new polygon is controlled by the two parameters η and σ. The criteria of convergence (see details in Ref. [14]) can easily be determined theoretically by estimating the Hausdorff distance [16]. In simple cases such as hydrogen abstraction (presumed to be collinear) reactions, it is practical to start from a closed polygon (see Applications below). The fusion of the sides of the polygon into a curved line (i.e. into the converged RP) will then indicate the convergence of the procedure.

3. Applications

The MB-function [5] is formed by the linear combination of four simple exponential functions and it has three minima and two first-order SPs; therefore, it is very suitable for testing RP-following algorithms. As a starting curve we chose a straight line determined by the points $(-2;2)$ and $(2;-2)$ in such a way that it crossed broadly the steep and curved surface (top view, Fig. 1(a), curve 1). We found that the determination of the IRC could be facilitated and accelerated by taking into account this special case, e.g. $\log(160+U)$ in place of U. The "RP" determined by this function lies in a deep and winding canyon. Despite the rather rough choice, far from ideal, our algorithm easily "followed" the path and the successive sets of approximate curves 1–6, converging rapidly to the true sought-after path; it reached practical convergency in the 57th step, the run time being 1354 s.[d] The surface showing the stroboscopic view of the IRC with the time-resolved evolution polygons in the canyon is displayed in Fig. 1(b) (curves 1–6; rotation about the z-axis: 40°, tilt after rotation: 20°).

The GS-function [12] is quite interesting from another point of view in comparison with the MB-function; now the analytical form of the meta-IRC is known: $y=\sin x$, and the RP has neither minima nor SPs. Starting from a straight line defined by the points $(0;0)$ and $(0;2)$ (Fig. 2(a), curve 1) and fixing its one end[e] at the origin, we determined the evolution phases of the RP (see Fig. 2(a), curves 1–3). Since following the meta-IRC described by the GS-function, the function value is decreasing monotonously, and only a certain part of the infinite symbolic RP can be reproduced (Fig. 2(a), curve 3). In each cycle of iterations we passed over beyond the periodically recurring regions $[0,2\pi]$ when following the RP. When continuing the procedure, increasingly longer parts of the RP could be determined; therefore, down from the fixed origin the successive approximate curves reproduced the RP in arbitrary lengths (the arrows in Fig. 2(a) show the approximate numbers of iteration steps and run times). Note that in similar cases the length of the initial polygon could be reduced at any rate and the whole RP would still be reproduced. In our case this means that starting from a digon defined by the points $(0;0)$ and $(x_0;0)$ (for any $x_0>0$) and fixing its one end at the origin,

[c] Without homogenization the RP would separate into parts.

[d] By using identical parameter values, the IRC of the unmodified MB-function U could not be determined at all. Reducing drastically the values of the controlling parameters, the IRC can obviously be determined but at the price of much longer run times and a much higher cost of computation. In Ref. [21] we will show the technique for these modifications and their consequences in the gain of computational time.

[e] If this is not done then the sine wave, like a streamlet varying in length, would wimple along further down in the narrow, deep canyon hollowed in the surface (Fig. 2(c)).

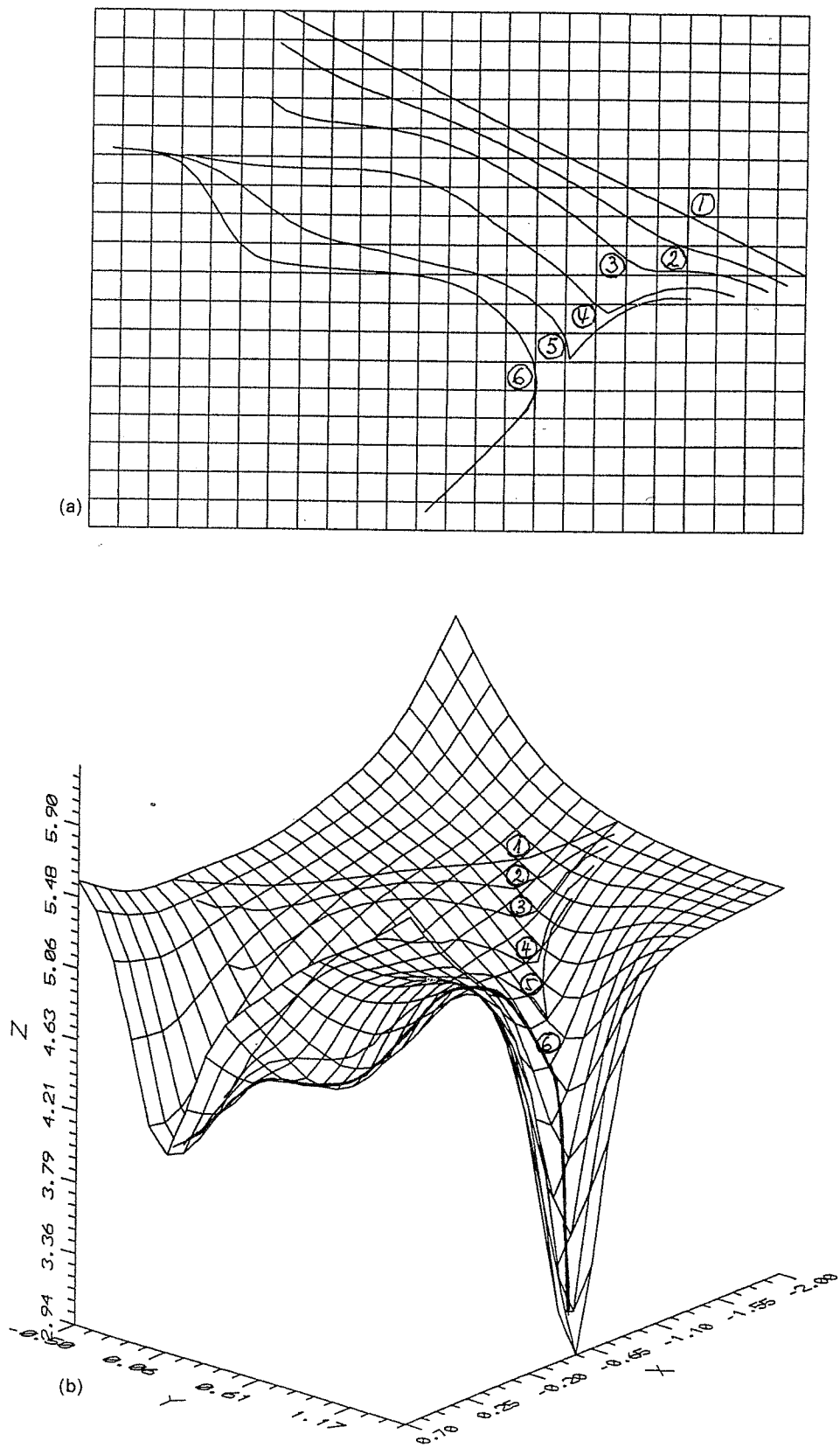

Fig. 1. (a) Plan-view of the Müller–Brown surface showing evolution phases (1–6) of the RP started from a digon. (b) Stroboscopic view of the time-resolved RP embedded in the Müller–Brown surface profile.

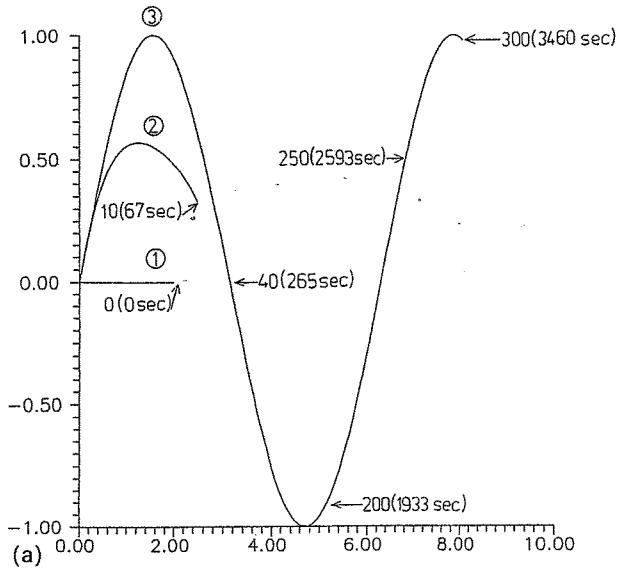

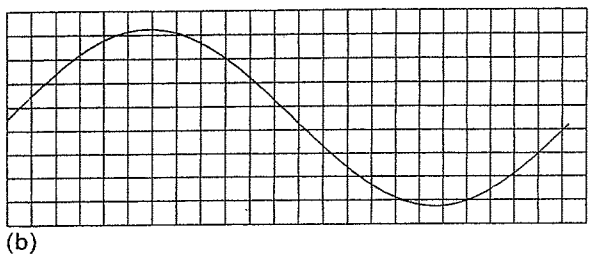

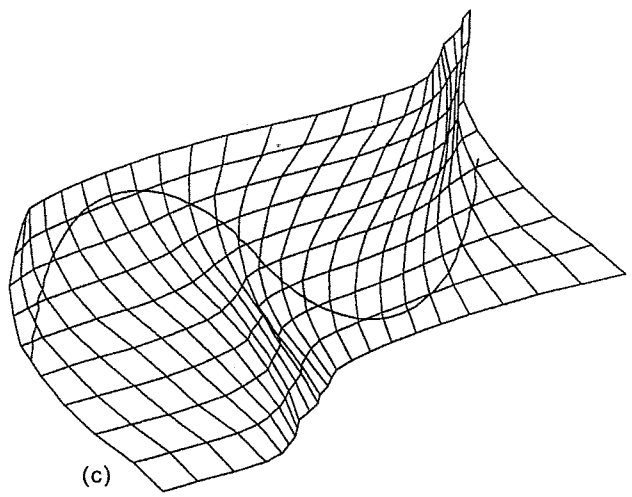

Fig. 2. (a) The time-resolved Gonzales–Schlegel RP started from a digon. Arrows on the curves show numbers of iterations and corresponding run times of some evolution phases. (b) Plan-view of the Gonzales–Schlegel surface showing the sinusoidal RP. (c) Side-view of the Gonzales–Schlegel surface profile with the sinusoidal RP.

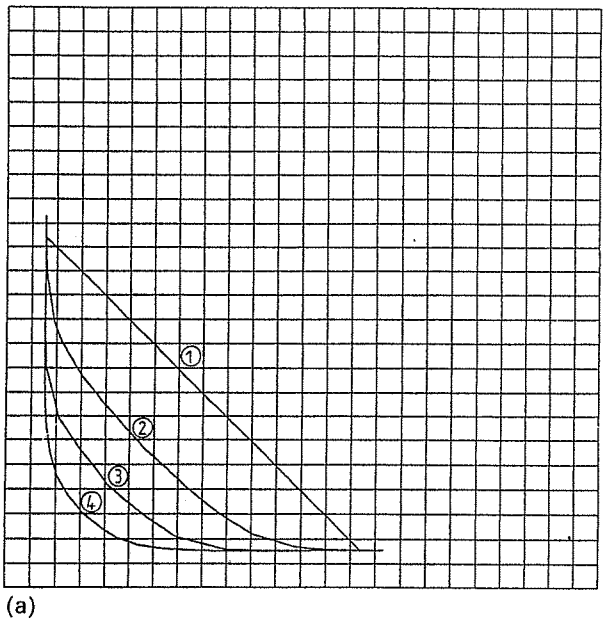

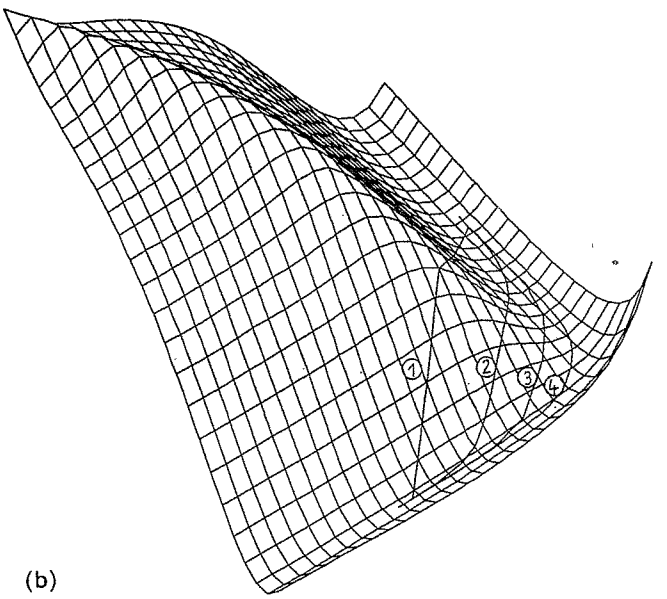

Fig. 3. (a) Plan-view of the $H_2 + H$ reaction surface showing the time-resolution of the RP starting from a digon. (b) Side-view of the H_3 surface profile with the evolution phases of the IRC starting from a digon.

the periodical parts of the RP can be reproduced at any length. Since the starting point can be chosen anywhere, any part of the infinitely long RP can easily be determined by the DDRP algorithm. Figures 2(b) and 2(c) display a section of the RP on the plane and on the crumpled (rotation about z-axis: 165°, tilt after rotation: 65°) GS-surface, respectively. Starting from a digon defined by the

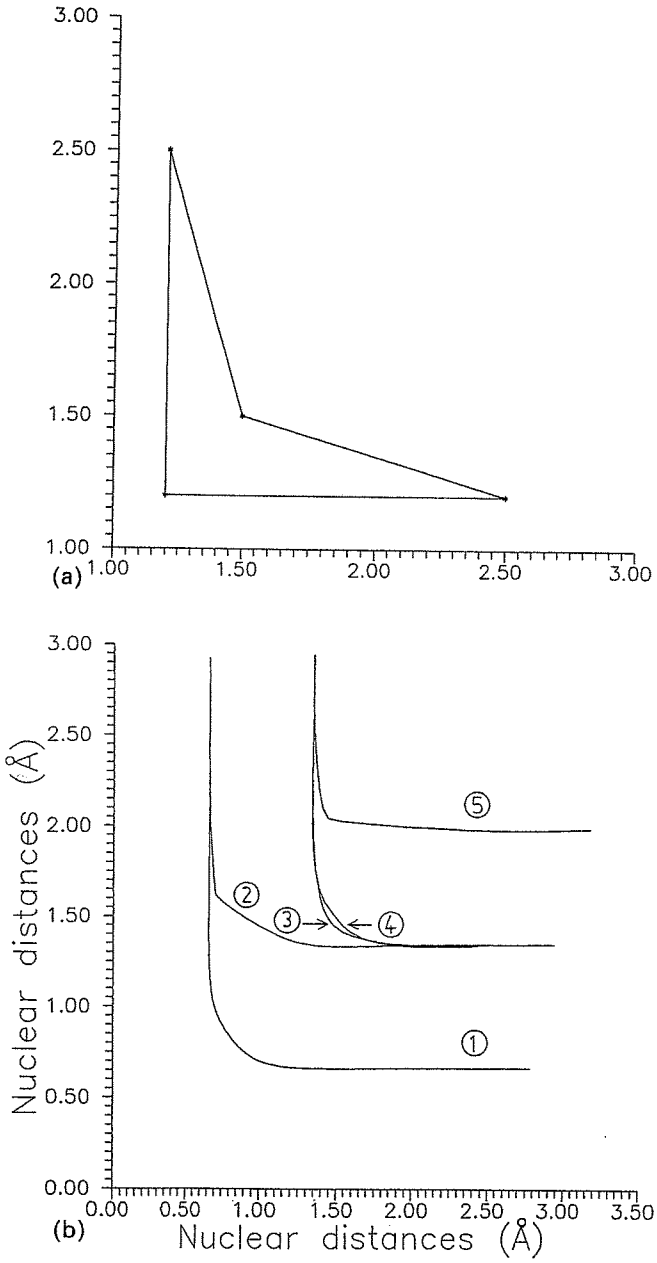

Fig. 4. (a) Starting tetragon for the chemical reactions $H_2 + H$, $H + HCl$, $HCl + H$, $Cl + HCl$ and $HCl + Cl$. (b) Converged RPs for the chemical reactions 1: $H_2 + H$, 2: $H + HCl$, 3: $HCl + H$, 4: $Cl + HCl$, 5: $HCl + Cl$.

points (0.66, 2.00) and (2.00, 0.66), approximate time-resolved IRC curves for the $H_2 + H$ reaction were computed and embedded in the PES of the H_3 system (top view and surface profile are shown in Figs. 3(a) and 3(b), curves 1–4). In order to make easy comparisons in the evolution curves and run times for the different chemical examples the same closed tetragon (Fig. 4(a)) defined by the

Table 1
Comparisons of step numbers and run times for some collinear reactions

Reaction	Convergence in the iteration	
	Number of steps	Time (s)
1. HH + H	4	3460
2. HH + Cl	10	29286
3. HCl + H	6	8463
4. ClH + Cl	21	68719
5. HCl + Cl	25	125268

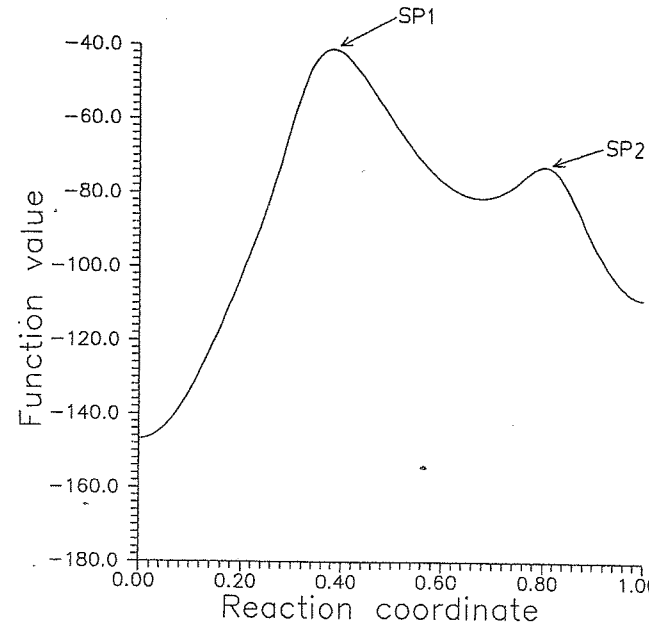

Fig. 5. The Müller–Brown RP indicating saddle points in the representation of function value vs. reaction coordinate.

points (1.20, 1.20), (1.20, 2.50), (1.50, 1.50) and (2.50, 1.20) was also used to start with. The converged RPs are displayed in Fig. 4(b), curves 1–5 for the systems $H_2 + H$, $H + HCl$, $HCl + H$, $Cl + HCl$ and $HCl + Cl$ computed as collinear reactions.[f] The number of iteration steps and the corresponding convergence run times are summarized in Table 1. As by-products of searchings for RPs, one can, of course, easily obtain plots of energy vs. reaction co-ordinate and energy vs. nuclear distances with arbitrary accuracy (see

[f] Computational results for the same systems allowing deviations from collinearity are also described in Ref. [22].

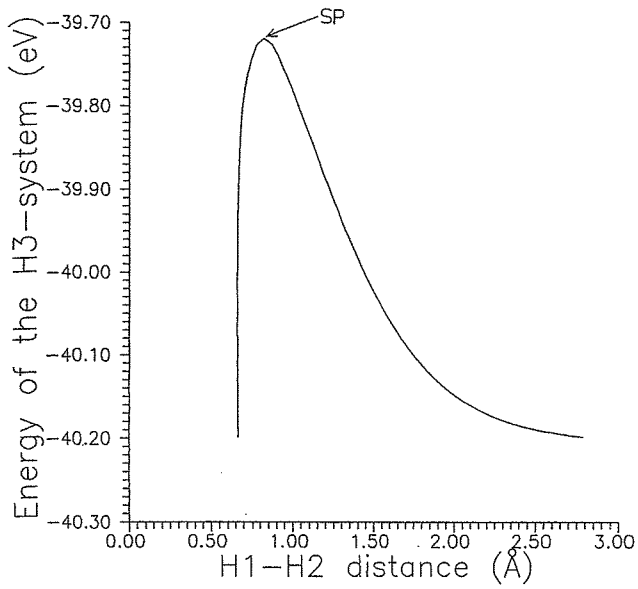

Fig. 6. The $H_2 + H$ RP indicating saddle point in the representation of energy (eV) vs. nuclear distance (Å).

Figs. 5 and 6 for the MB-function and the $H_2 + H$ reaction, respectively). By using the MNDO [23] quantum chemical approximation the computations were carried out by an IBM compatible AT 286 PC equipped with an 80287 mathematical coprocessor.[g]

4. Supplementary material

Individual evolution polygons, stroboscopic views and time-resolution curves for the examples, etc. can be obtained on request from the authors.

Acknowledgements

The authors thank Dr. T. Körtvélyesi for valuable discussions and advice. This work was supported by the Hungarian Scientific Research Fund (Grant No. OTKA: T 4202).

[g] The use of the DDRP procedure is not limited to the employment of a semiempirical quantum chemical method. Ab initio or even classical methods suitable for calculating the total energy of a system can equally be used in connection with the procedure. Our choice was influenced by the requirements concerning simplicity, ease and rapidity.

References

[1] C.P. Baskin, C.F. Bender, C.W. Bauschlicher, Jr., and H.F. Schaefer III, J. Am. Chem. Soc., 96 (1974) 2709.
[2] J.W. McIver and A. Komornicki, J. Am. Chem. Soc., 96 (1974) 5798.
[3] P. Pechukas, J. Chem. Phys., 64 (1976) 1516.
[4] K. Ishida, K. Morokuma and A. Komornicki, J. Chem. Phys., 66 (1977) 2153.
[5] K. Müller and L.D. Brown, Theor. Chim. Acta, 53 (1979) 75.
[6] W.L. Hase and R.J. Duchovic, J. Chem. Phys., 83 (1985) 3448.
[7] M.W. Schmidt, M.S. Gordon and M. Dupuis, J. Am. Chem. Soc., 107 (1985) 2585.
[8] P.G. Jasien and R. Shepard, Int. J. Quantum Chem., Symp., 22 (1988) 183.
[9] M. Page and J.W. McIver, J. Chem. Phys., 88 (1988) 922.
[10] C. Gonzalez and H.B. Schlegel, J. Chem. Phys., 90 (1989) 2154.
[11] C. Gonzalez and H.B. Schlegel, J. Phys. Chem., 94 (1990) 5523.
[12] C. Gonzalez and H.B. Schlegel, J. Chem. Phys., 95 (1991) 5853.
[13] L.L. Stachó and M.I. Bán, Theor. Chim. Acta, 83 (1992) 433.
[14] L.L. Stachó and M.I. Bán, J. Math. Chem., 11 (1992) 405.
[15] L.L. Stachó and M.I. Bán, Theor. Chim. Acta, 84 (1993) 535.
[16] L.L. Stachó and M.I. Bán, Comput. Chem., 17 (1993) 21.
[17] Gy. Dömötör, L.L. Stachó and M.I. Bán, QCPE program, in press.
[18] Gy. Dömötör, M.I. Bán and L.L. Stachó, J. Comput. Chem., 14 (1993) 1491.
[19] K. Fukui, Acc. Chem. Res., 14 (1981) 363.
[20] E. Kraka and T.H. Dunning, Jr., in Advances in Molecular Electronic Structure Theory, Vol. 1, JAI Press, Greenwich, CT, 1990, p. 147.
[21] Gy. Dömötör, M.I. Bán and L.L. Stachó, J. Chem. Soc., Faraday Trans., in press.
[22] Gy. Dömötör, T. Körtuélyesi, L.L. Stachó and M.I. Bán, J. Comput. Chem., in press.
[23] W. Thiel, QCPE program #353, MNDO: Molecular Orbital calculations by the MNDO Method with Geometry Optimization, QCPE Bull., 10 (1978) 353.